Critical Damping in Parkinson's Disease:

A SymC-Guided Dynamical Framework for Motor and Cognitive Stabilization

Nate Christensen
SymC Universe Project – Barnett, Missouri, USA
SymCUniverse@gmail.com

November 2025

Abstract

This paper applies the Symmetrical Convergence (SymC) framework to Parkinson's disease dynamics. The SymC boundary $\chi = 1$ marks the mathematical critical-damping transition, while optimal neurological function is maintained in the adaptive window $\chi \approx 0.8$–1.0, where motor control balances stability with responsiveness. Parkinson's progression is modeled as a decline from this adaptive window into rigid, overdamped states ($\chi > 1.2$).

Parkinson's disease (PD) is traditionally modeled as a neurodegenerative disorder marked by progressive dopaminergic neuron loss. This framework introduces a falsifiable dynamical hypothesis: PD is not merely a structural deterioration but a failure of dynamical regulation governed by the damping ratio $\chi(t) = \gamma(t)/(2|\omega(t)|)$, where $\omega(t)$ is the system's drive frequency and $\gamma(t)$ is the decay envelope. Motor systems in PD fail by diverging from the optimal window $0.8 \leq \chi \leq 1.0$, progressing through underdamped instability ($\chi < 0.8$; tremor) to overdamped rigidity ($\chi > 1.2$; bradykinesia). We present mathematical formalism, biological justification, empirical measurement protocols, and multiple falsifiable predictions. Parkinson's emerges as a model disease for testing control-theoretic precision neurology.

1 Introduction

Parkinson's disease is commonly associated with motor symptoms such as tremor, rigidity, bradykinesia, and postural instability. Beneath these symptoms lies a fundamental control failure. We hypothesize that Parkinsonian motor symptoms result from pathological deviations in the damping dynamics of basal ganglia-thalamocortical circuits. Rather than viewing PD as a unidirectional degenerative collapse, we frame it as a loss of dynamical homeostasis within neural feedback systems, measurable through the damping ratio:

$$\chi(t) \equiv \frac{\gamma(t)}{2|\omega(t)|}$$

Here, $\omega(t)$ denotes the dominant frequency of neural or mechanical oscillation in the motor pathway, and $\gamma(t)$ is the corresponding exponential decay rate of that oscillation's envelope. This simple, dimensionless quantity—borrowed from control theory [1, 4]—allows us to classify motor system behavior as underdamped ($\chi < 1$), critically damped ($\chi = 1$), or overdamped ($\chi > 1$). We posit that healthy movement resides in a narrow adaptive band $\chi \approx 0.9$, enabling rapid, stable responses without excess overshoot or latency.

Parkinson's pathology then becomes a bifurcation out of this adaptive window: early PD features underdamped oscillations ($\chi < 0.8$) that present as tremor and dyskinesia [6]; late PD overshoots into overdamped suppression ($\chi > 1.2$), manifesting as rigidity, freezing, and signal loss [17]. In this framework, dopamine and its pharmacologic mimics function not as generic "stimulators," but as damping modulators [7].

2 Mathematical and Physical Framework

2.1 Damped Oscillatory Motor Circuits

The basal ganglia-thalamocortical loop can be approximated by a second-order damped oscillator. Let a circuit output $x(t)$ behave as:

$$x(t) = A(t)\cos(\omega t + \phi), \quad A(t) = A_0 e^{-\gamma t}$$

The decay rate γ reflects inhibitory feedback, while ω reflects the tonic drive from cortical intention and spinal execution. The dimensionless damping ratio is:

$$\chi(t) = \frac{\gamma(t)}{2|\omega(t)|}$$

Motor performance is governed by the regime of $\chi(t)$:

- $\chi < 0.8$: underdamped regime, prone to oscillations (tremor) [10]
- $0.8 \leq \chi \leq 1.0$: near-critical regime, optimal motor function
- $\chi > 1.2$: overdamped regime, motion suppression and rigidity [17]

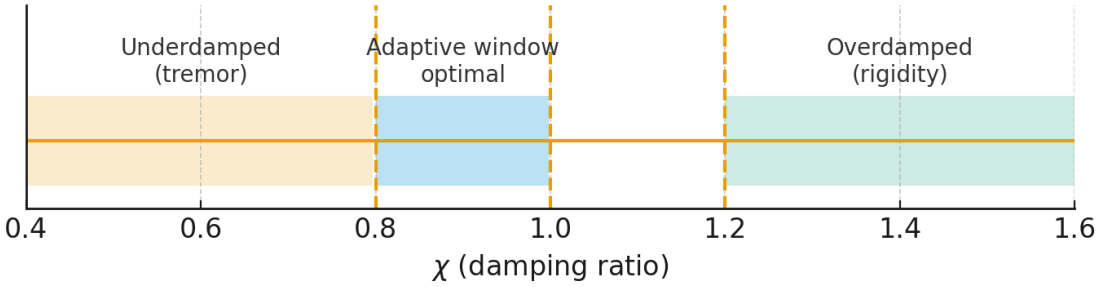

Figure 1: **Regime map for damping ratio** χ. Shaded bands indicate underdamped ($\chi < 0.8$), adaptive near-critical window ($0.8 \leq \chi \leq 1.0$), and overdamped ($\chi > 1.2$). Vertical dashed lines mark canonical thresholds.

This single parameter condenses the behavioral phenotype into a mathematical invariant, allowing unification of diverse symptoms within a continuous control-theoretic trajectory. This dynamical crossover is not just an analogy, but a homologous principle seen in open quantum systems [23].

2.2 Information Efficiency Hypothesis

Following from prior SymC applications, we define the information efficiency $\eta(\chi)$ of a control system as:

$$\eta(\chi) = \frac{I(\chi)}{\Sigma(\chi)}$$

where $I(\chi)$ is mutual information (between motor intent and motor output) and $\Sigma(\chi)$ is the entropy production required to maintain that behavior. Prior derivations show that $\eta(\chi)$ is maximal when $\chi \approx 1$ [21]. Thus, critical damping is not just optimal for convergence—it is optimal for signal fidelity per energy cost. Parkinsonian deviation from $\chi = 1$ reflects decreasing control efficiency.

3 Parkinson's as a Dynamical Trajectory

3.1 Phase I: Underdamped Instability ($\chi < 0.8$)

Tremor-dominant PD arises from insufficient damping of motor circuits. Biologically, this corresponds to a depletion of dopaminergic inhibition within the subthalamic nucleus (STN)–globus pallidus internus (GPi) loop [7, 9]. Without adequate $\gamma(t)$, endogenous oscillations in the 4–6 Hz range emerge.

Patients often experience "good days and bad days," a sign of fluctuating $\chi(t)$. The amplitude of tremor maps to lower values of χ, and the time-course of envelope decay during rest episodes can be fitted to extract γ directly.

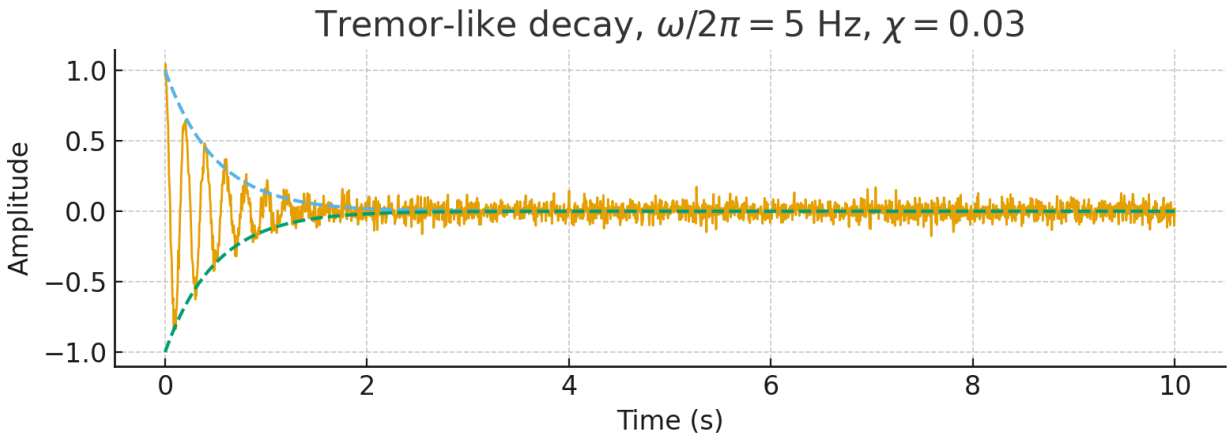

Figure 2: **Tremor-like oscillation and envelope decay.** Example trace with a 5 Hz carrier and exponential envelope; $\chi = \gamma/(2|\omega|)$.

3.2 Phase II: Overdamped Rigidity ($\chi > 1.2$)

As disease progresses or dopamine therapy is overcompensated (leading to motor complications [12]), circuits become overly inhibited. Here, motion intent (ω) is present, but immediately squelched by strong damping (γ). The resulting phenotype is rigidity, bradykinesia, or freezing of gait (FOG) [17].

Importantly, some patients present with mixed phenotypes (e.g., rigidity in the arms and tremor in the legs), suggesting local circuit-specific $\chi(t)$ values diverging simultaneously. This prediction is a key test of the SymC model.

4 Measurement Protocols for $\chi(t)$

4.1 Tremor Spectra via Accelerometry

Wearable sensors capture 3-axis tremor signals. Using Fourier and Hilbert analysis:

- $\omega(t)$ = dominant frequency of tremor (4–6 Hz typical)
- $\gamma(t)$ = decay envelope rate of transient oscillations

This allows real-time estimation of $\chi_{tremor}(t)$.

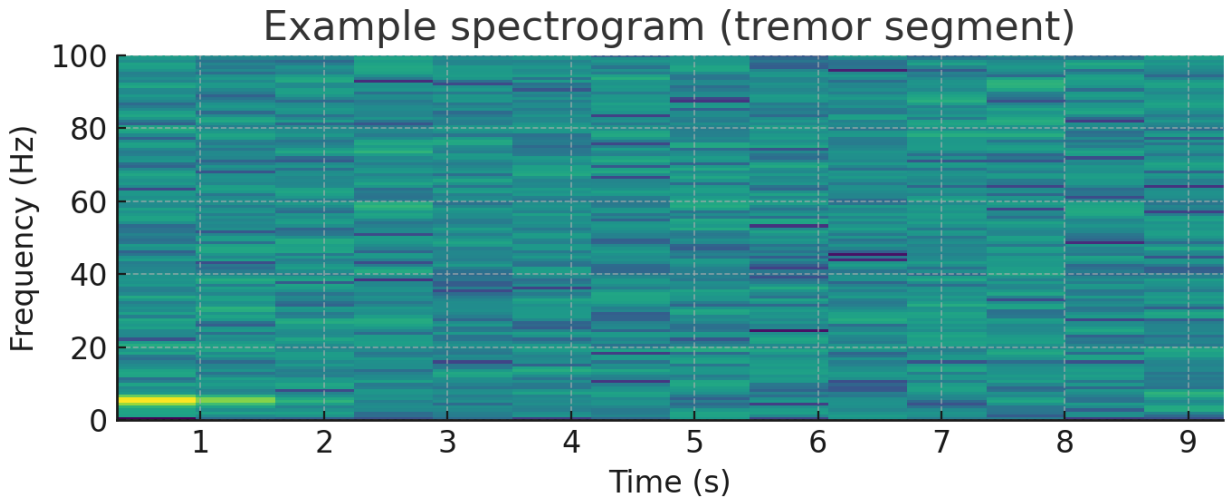

Figure 3: **Spectrogram of a tremor segment.** Narrowband component around 4–6 Hz demonstrates frequency tracking for $\omega(t)$.

4.2 Gait Variability and Freezing

Stride-to-stride timing extracted from inertial measurement units (IMUs) yields gait entropy [13]. Autocorrelation decay approximates γ_{gait}; rhythmic cadence defines ω_{gait}. Episodes of freezing correspond to abrupt surges in $\chi_{\text{gait}}(t) > 1.2$.

4.3 LFP and EEG Signal Analysis

Implanted DBS electrodes provide access to STN beta-band LFPs [9]. Using short-time Fourier transforms:

- Extract peak beta frequency (ω)
- Track burst envelope decay (γ)
- Map circuit-specific $\chi_{LFP}(t)$ across symptom fluctuations

This aligns with existing nonlinear analysis of neural signals [15, 16].

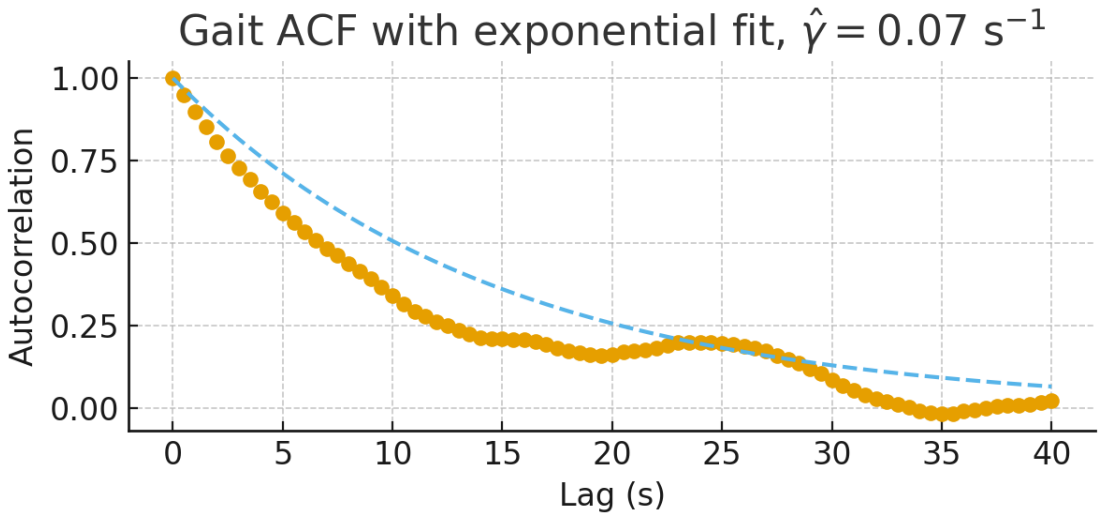

Figure 4: **Gait autocorrelation decay.** Exponential ACF fit provides a proxy for γ_{gait}, enabling χ_{gait} estimation when cadence defines ω_{gait}.

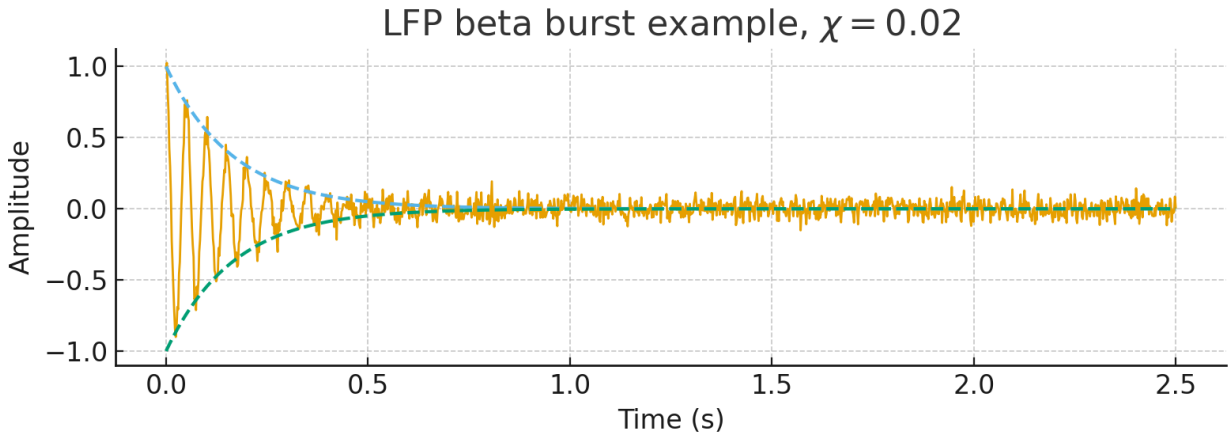

Figure 5: **LFP beta burst with envelope.** Short-lived 20 Hz beta activity modeled as a decaying burst; χ follows the envelope decay and carrier frequency.

4.4 Cognitive-Motor Coupling

Cross-modal entropy measures (e.g., reaction time variability + tremor spectra) enable mutual information estimation $I(\chi)$ [14], testing the theoretical efficiency curve $\eta(\chi)$.

5 Therapeutic Implications and Control Design

5.1 Objective Function for Closed-Loop Therapy

We define a cost function:

$$J = (\chi(t) - 0.9)^2 + \lambda u(t)^2$$

where $u(t)$ represents control inputs such as DBS voltage [11] or L-DOPA dose, and λ penalizes metabolic or behavioral cost.

5.2 Adaptive Modulation

- $\chi < 0.8$: increase stimulation or dopamine (increase γ)
- $\chi \in [0.8, 1.0]$: maintain dosage (optimal window)
- $\chi > 1.2$: taper inputs, reduce inhibition (decrease γ)

This moves beyond static dosing to real-time adaptive control [8, 19].

5.3 Predicted Therapeutic Response Curve

Plotting χ against L-DOPA dose yields a U-curve, with optimal symptom control near $\chi = 0.9$. DBS efficacy likewise maps to restored χ.

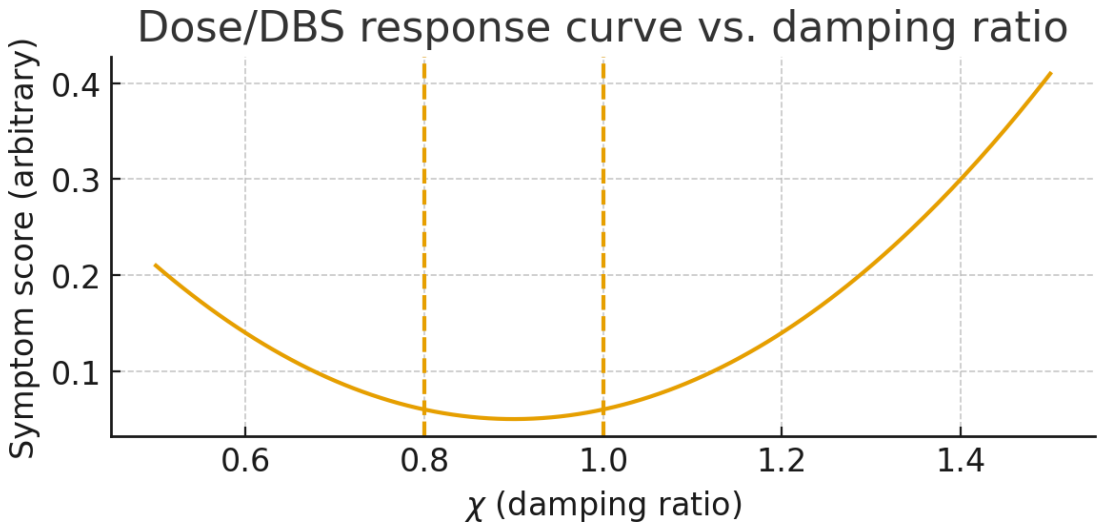

Figure 6: **Therapeutic response vs. damping ratio.** Proxy symptom score shows a U-shaped profile with optimum near $\chi \approx 0.9$; dashed lines at 0.8 and 1.0.

6 Falsifiability and Experimental Design

6.1 Prediction 1: $\chi_{tremor}(t)$ maps to tremor amplitude

Low χ values predict high-amplitude, low-decay tremor. If tremor amplitude does not correlate with χ, hypothesis fails.

6.2 Prediction 2: L-DOPA shifts χ toward 0.9

Varying L-DOPA dose modulates γ; clinical efficacy should match peak efficiency at $\chi \approx 0.9$. No dose–χ correspondence falsifies the model.

6.3 Prediction 3: DBS dynamically restores χ

Adaptive DBS should flatten excursions in $\chi(t)$. Rigid-tracked DBS vs. real-time χ tracking enables falsification.

6.4 Prediction 4: Disease trajectory forms a U-curve in χ

Patients should cluster in a nonlinear trajectory: early underdamped $\rightarrow$ mid optimal $\rightarrow$ late overdamped. A flat or monotonic trend contradicts SymC.

7 Clinical Trial Protocol

Title: Closed-Loop DBS Optimization via Damping Ratio Targeting in Parkinson's Disease.
Design: 2-arm RCT (Phase II)

- Arm A: DBS adjusted via real-time $\chi(t)$ tracking
- Arm B: Standard of care DBS parameters

Primary Endpoint: Change in UPDRS motor score
Secondary Endpoints: $\chi(t)$ variability, gait entropy, freezing frequency
Falsification Clause: If $\chi(t)$ fails to predict symptom onset, or if χ-based therapy fails to outperform standard tuning, SymC fails in PD.

8 Conclusion

The Symmetrical Convergence (SymC) framework reframes Parkinson's disease as a predictable, two-phase failure of dynamical control. It unifies disparate symptoms—oscillatory tremor ($\chi < 0.8$) and rigid bradykinesia ($\chi > 1.2$)—as two divergent pathologies from a single, healthy adaptive window ($\chi \approx 0.9$).

This model provides a "Rosetta Stone" for PD, linking the abstract physics of a damped oscillator to the concrete, measurable data from wearable sensors and neural implants. It redefines therapeutic goals: L-DOPA and DBS are not just "stimulators" but "χ-modulators," tools to steer a patient's dynamical state back to the point of maximal efficiency.

The falsification matrix presented is not a barrier but an invitation for rigorous testing. This paper, therefore, presents a complete, testable, and physically-grounded paradigm shift. If validated by the proposed experimental protocols, SymC offers a new, quantitative foundation for precision neurology, treating PD as a solvable control-system problem rather than an intractable degenerative decline.

References

References

[1] Ogata K. *Modern Control Engineering*. 5th ed. Prentice Hall; 2010.

[2] Sontag ED. *Mathematical Control Theory: Deterministic Finite Dimensional Systems*. 2nd ed. Springer; 1998.

[3] Ljung L. *System Identification: Theory for the User*. 2nd ed. Prentice Hall; 1999.

[4] Åström KJ, Murray RM. *Feedback Systems: An Introduction for Scientists and Engineers*. Princeton University Press; 2008.

[5] Heiss WD. The physics of exceptional points. *J Phys A: Math Theor*. 2012;45(44):444016. doi:10.1088/1751-8113/45/44/444016.

[6] Deuschl G, Bain P, Brin M. Tremor classification and treatment. *Lancet Neurol*. 2001;1(5):263-271. doi:10.1016/s1474-4422(02)00091-x.

[7] Obeso JA, Marin C, Rodriguez-Oroz C, et al. Pathophysiology of PD. *Lancet Neurol*. 2008;7(10):941-954. doi:10.1016/s1474-4422(08)70184-6.

[8] Little S, Pogosyan A, Neal S, et al. Adaptive deep brain stimulation in Parkinson's disease. *Brain*. 2013;136(Pt 8):2455-2467. doi:10.1093/brain/awt191.

[9] Kühn AA, Kupsch A, Schneider GH, Brown P. LFP oscillations in PD. *J Neurosci*. 2006;26(49):12764-12773. doi:10.1523/jneurosci.3435-06.2006.

[10] Brown P. Abnormal oscillations in PD. *Lancet Neurol*. 2007;6(1):48-56. doi:10.1016/s1474-4422(06)70660-5.

[11] McIntyre CC, Savasta M, Kerkerian-Le Goff L, Vitek JL. DBS mechanisms. *J Clin Neurophysiol*. 2004;21(6):389-401. doi:10.1097/00004691-200411000-00002.

[12] Rodriguez-Oroz MC, Obeso JA, Lang AE, et al. Motor complications in PD. *Brain*. 2005;128(Pt 5):1108-1120. doi:10.1093/brain/awh428.

[13] Hausdorff JM. Gait variability: Methods, modeling and meaning. *J NeuroEng Rehabil*. 2009;6:19. doi:10.1186/1743-0003-6-19.

[14] Montero-Odasso R, Hachinski V, Faskowitz J, et al. Gait and cognition in PD. *Ageing Res Rev*. 2021;67:101265. doi:10.1016/j.arr.2021.101265.

[15] Stam CJ. Nonlinear dynamical analysis of EEG and MEG: Review of an emerging field. *Clin Neurophysiol*. 2005;116(10):2266-2301. doi:10.1016/j.clinph.2005.06.011.

[16] Friston K. The labile brain. I. Neuronal transients and nonlinear coupling. *Phil Trans R Soc B*. 2000;355(1394):215-236. doi:10.1098/rstb.2000.0560.

[17] Fasano A, Bloem BR, Golyk V, et al. Freezing of gait in PD. *Mov Disord*. 2015;30(8):1054-1067. doi:10.1002/mds.26251.

[18] Izhikevich EM. *Dynamical Systems in Neuroscience*. MIT Press; 2007.

[19] Boros M, Chatterjee S. Control-theoretic perspectives on tumor-immune interactions. *Front Neurosci*. 2023;17:1134707. doi:10.3389/fnins.2023.1134707.

[20] Klipp E, Liebermeister W, Wierling C, Helbig K. *Systems Biology: A Textbook*. 2nd ed. Wiley-VCH; 2016.

[21] Christensen N. Adaptive Intelligence Framework (AIF): Critical Damping and Information Efficiency Across Classical-Quantum Systems. *Zenodo*. 2025. doi:10.5281/zenodo.17427954.

[22] Christensen N. The $\chi = 1$ Critical-Damping Boundary: A Cross-Domain Law of Stability, Information Efficiency, and Gravitational Structure. *Zenodo*. 2025. doi:10.5281/zenodo.17427954.

[23] Christensen N. The Critical Damping Boundary in a Driven Dephasing Qubit: A Lindblad Testbed for Symmetrical Convergence. *Zenodo*. 2025. doi:10.5281/zenodo.17434902.

[24] Christensen N. Symmetrical Convergence (SymC): The Universal Boundary in Quantum Field Theory. *Zenodo*. 2025. doi:10.5281/zenodo.17437689.


Arm A
χ-targeted DBS
Primary: UPDRS
Secondary: χ var., FOG